ACS Sustainable Chemistry & Engineering

Letter

pubs.acs.org/journal/ascecg

Water-Catalyzed Low-Temperature Transformation from Amorphous to Semi-Crystalline Phase of Ordered Mesoporous Titania Framework

Karine Assaker,[†] Cédric Carteret,[‡] Bénédicte Lebeau,[§] Claire Marichal,[§] Loïc Vidal,[§] Marie-José Stébé,[†] and Jean-Luc Blin[†,*]

[†]Université de Lorraine/CNRS, SRSMC, UMR7565, F-54500 Vandoeuvre-lès-Nancy, France

[‡]Université de Lorraine/CNRS, LCPME, UMR7564, F-54600 Villers-lès-Nancy, France

[§]Université de Haute Alsace (UHA), CNRS, Equipe Matériaux à Porosité Contrôlée (MPC), Institut de Science des matériaux de Mulhouse (IS2M), UMR 7361, ENSCMu 3bis rue Alfred Werner F-68093, Mulhouse cedex, France

Supporting Information

ABSTRACT: In this paper, the phase transformation in water at low temperature from amorphous TiO_2 to semi-crystalline anatase is reported. Our approach is an environmentally friendly low energy consumer process that requires no specific devices or instrumentation. The phase transition occurs even at room temperature. However, the higher the temperature is, the better the crystallinity is. Crystallization of amorphous titania occurs through a rearrangement of the TiO_6^{2-} octahedral units in amorphous TiO_2. The phase transformation is catalyzed by water, which adsorbs on the titania surface to form bridges between the surface OH groups of different octaedra. The obtained titania samples have been used for the photodegradation of methyl orange. Because of the formation of anatase, mesoporous TiO_2 exhibits a photocatalytic activity after treatment in water. However, the activity is lower than that of the standard photocatalysts because the TiO_2 treated during 1 h in water at 120 °C has degraded 85% of methyl orange within 240 min compared to 45 min for P25.

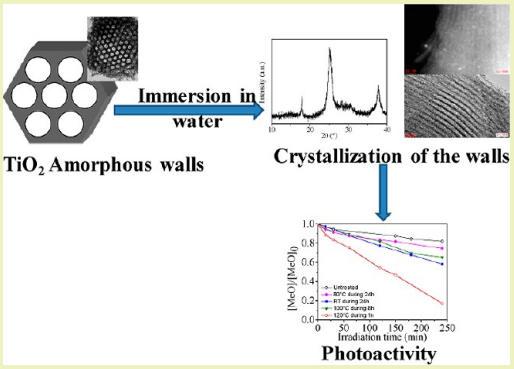

KEYWORDS: *Ordered Mesoporous Titania, Water treatment, Phase Transformation, Amorphous, Anatase*

INTRODUCTION

Because of their applications in energy conversion and storage, catalysis, sensing, adsorption, and separation, ordered mesoporous oxides such as SiO_2, ZrO_2, Al_2O_3 have attracted much attention for the past few years.[1,2] Among them, titania is of particular interest for applications in electronics and electrochemical systems, including photoelectrochemical solar cells, electrocatalysis, optoelectronic sensors devices, and high performance photocatalytic films.[3−7] The photocatalytic activity of TiO_2 is one of its distinctive features, mainly attributed to its anatase phase,[8,9] and it is reported that higher crystallinity enhanced drastically the photocatalytic activity of TiO_2 materials.[10,11] In addition to crystallinity, the efficiency of the photocatalyst will also depend on its specific surface area. From this point of view, mesoporous TiO_2 is an excellent candidate for this application.[12,13] Two mechanisms can lead to the formation of these ordered TiO_2 mesostructures.[14] The first way is the soft templating pathway that implies co-assembly of the titania precursor and surfactant, similar to the preparation of ordered mesoporous silica.[15−23] However, using the templated synthesis, TiO_2 with amorphous walls are usually recovered. The crystalline structure is obtained after heating the material at higher temperature, but this process is often responsible for the collapse of the framework. The second way to prepare ordered mesostructures is the hard-templating method. In that case, the mesoporous titania is prepared in a confined space, for example, via replication of mesoporous silica as a hard template. Because the template prevents collapse of the mesostructure upon calcination, the main advantage of this method is the preservation of the ordered mesopore channel array during the crystallization step at high temperature. However, this pathway is time consuming (long process), not environmentally friendly, and can require specific devices and instrumentation. The transformation of an amorphous wall into a semi-crystalline framework without the collapse of the mesostructure by a simple, low energy, and environmentally friendly way is therefore still a challenge. In this paper, we demonstrate that the amorphous walls of ordered mesoporous TiO_2 can be transformed into semi-crystalline anatase framework by a simple, green, and low temperature treatment in water.

Received: August 29, 2013
Revised: October 7, 2013
Published: October 8, 2013

MATERIALS AND METHODS

Preparation of Amorphous Ordered Mesoporous Titania. Mesoporous titania have been prepared and characterized according to the procedure we have previously reported.[22,23] The obtained mesoporous titania materials have amorphous walls.

Anatase Formation. To carry out this study, 3 g of as-synthesized mesoporous titania were placed in deionized water at room temperature or refluxed at 80, 100, or 120 °C under stirring. After various immersion times, solutions were filtered. The samples were dried and analyzed.

Photocatalytic Activity. Methyl orange (Aldrich) was used as a model dye. Analyses have been performed according to the procedure we have previously reported.[24] The error on the measurement is estimated to 5%.

RESULTS AND DISCUSSION

As shown in Figure 1, the materials recovered after treatment in water at room temperature (RT) or at 80 °C adopt hexagonal

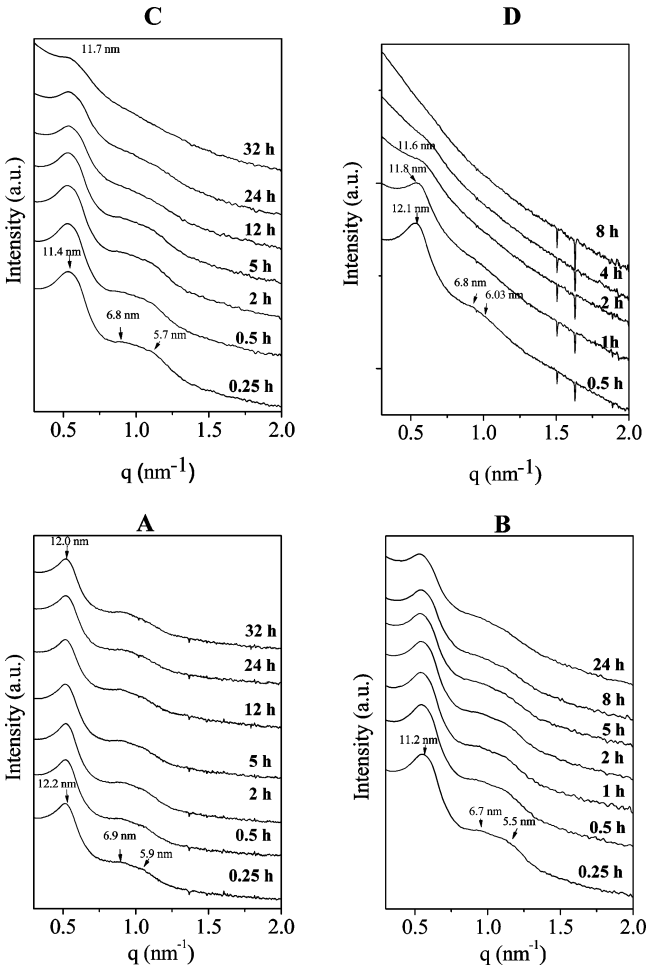

Figure 1. SAXS patterns of the started mesoporous titania and after immersion of TiO_2 in water during different times at room temperature (A), 80 (B), 100 (C) and 120 °C (D).

structure (Figure 1A and B). The (100), (110), and (200) reflections lines characteristic of the hexagonal array are detected at 12.2, 6.9, and 5.9 nm. The unit cell parameter a_0 ($a_0 = 2d_{100}/3^{1/2}$) is calculated to 14.1 nm after 0.25 h in water at RT. By increasing the temperature to 100 (Figure 1C) or 120 °C (Figure 1D), the secondary reflections disappear when the treatment in water is prolonged, meaning that disorganization of the mesopore network occurs. After treatment at 100 °C during 32 h, the presence of the main diffraction peak at 11.7 nm means that the mesopores are still present, but no organization exists. The higher the temperature is, the more pronounced the phenomenon is. At 120 °C after 8 h (Figure 1 D), no peak is observed on the SAXS patterns. In that case, collapse of the mesostructure has occurred, and the materials adopt a completely random-oriented pore structure. After treatment in water at room temperature according to the IUPAC classification,[25] the samples exhibit a type IV isotherm, characteristic of mesoporous materials (Figure S1A, Supporting Information). The isotherms exhibit a hysteresis in accordance with pore necking. The pore size distribution is rather narrow, and taking into account the error on the measurement, about 5%, we can consider that the pore diameter, determined by the BJH (Barret, Joyner, Halenda) method,[26] remains constant to about 9.0 nm (Figure S1A, insert, Supporting Information). The value of the specific surface area sharply reaches a plateau, about 340 m^2/g, after 15 h (Figure S2A, Supporting Information). A similar behavior is noted after treatment at 80 (S1B and S2B) or 100 °C (Figures S1C and S2C, Supporting Information). In addition no significant variation of the specific surface area is observed with an increase in temperature (Table 1).

By increasing the temperature to 120 °C, from Figure S1D of the Supporting Information, we can note that up to 1 h of treatment the shape of the isotherm and the pore size distributions are not modified. We can also consider that in

Table 1. Specific Surface Area, Pore Diameter, and Pore Volume of Mesoporous TiO_2 After Treatment in Water

temperature	duration (h)	specific surface area (m^2/g)	pore diameter (nm)	pore volume (cm^3/g)
room temperature	0.25	170	8.4	0.24
	0.5	258	8.6	0.37
	1	267	8.9	0.35
	2	270	8.9	0.37
	5	288	8.8	0.41
	8	305	9	0.33
	24	345	9	0.45
80 °C	0.25	278	8.4	0.44
	0.5	261	8.4	0.4
	1	259	8.6	0.38
	2	280	8.8	0.43
	5	301	8.3	0.45
	8	307	8.2	0.46
	24	356	8.4	0.51
100 °C	0.25	275	8.3	0.40
	0.5	300	9.3	0.51
	1	296	8.9	0.47
	2	319	9.3	0.48
	5	307	8.2	0.43
	8	318	8.3	0.36
	24	356	8.4	0.51
120 °C	0.25	422	9.1	0.52
	0.5	420	9.1	0.5
	1	289	8.4	0.21
	2	226	-	0.16
	5	234	-	0.17
	8	202	-	0.12
	24	149	-	0.09

dx.doi.org/10.1021/sc400323w | ACS Sustainable Chem. Eng. 2014, 2, 120−125

this period the pore diameter is unchanged. After 1 h at this temperature, the disorganization of the mesostructure detected by SAXS is also reflected by nitrogen adsorption−desorption analyses by both the spreading of the capillary condensation and the drop of the dV/dD values (Figure S1D, insert, Supporting Information). The pore size distribution is also broader. Until 1 h of treatment, the value of the specific surface area is in the same range as the one obtained after immersion in water at lower temperatures (Figure S2D, Supporting Information). Beyond 1 h of treatment, S_{BET} sharply decreases to reach 200 m^2/g after 8 h (Table 1). As a consequence, to keep the hexagonal pore ordering with a high specific surface area, the treatment in water at 120 °C of the mesostructure TiO_2 should not exceed 1 h.

In the range of 2θ, comprised between 10 and 40°, no peak is observed on the diffractogram of the untreated mesostructured titania (Figure 2). Upon treatment in water, the (101) and

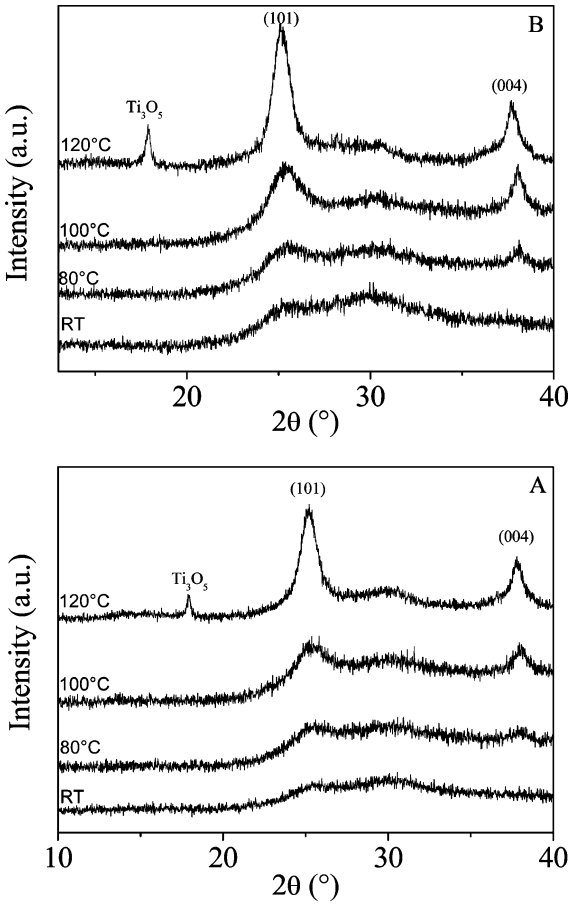

Figure 2. XRD patterns of mesoporous TiO_2 after immersion in water during 8 h (A) or 24 h (B) at different temperatures.

(004) reflections of anatase appear on the XRD patterns (Figure 2). The higher the temperature is, the higher the intensity and better the resolution of these reflections are. We can also observe that Ti_3O_5 appears after treatment at 120 °C. Using the Scherrer formula,[27] the mean size of the crystalline domains [$D = 0.9\ \lambda/(w \cos \theta)$, w is the width at half-maximum of the (101) peak] has been evaluated and the values are reported in Table 2. It is clear that bigger crystallites are obtained when the temperature or the immersion time in water is increased. For example, after 24 h, D varies from 4.2 to 8.7

Table 2. Variation of Coherent Domain Size of Anatase with Temperature

duration of immersion	room temperature	80 °C	100 °C	120 °C
8 h	–	3.5 nm	4.2 nm	6.9 nm
24 h	4.2 nm	4.3 nm	4.4 nm	8.7 nm

nm if the temperature is changed from room temperature to 120 °C. We can also note that the particles size is lower than 10 nm whatever the experimental conditions. The formation of anatase is further confirmed by Raman analysis. The typical vibrations of anatase[22,23] are detected on the Raman spectrum of commercial anatase (Figure 3, insert). As expected, no

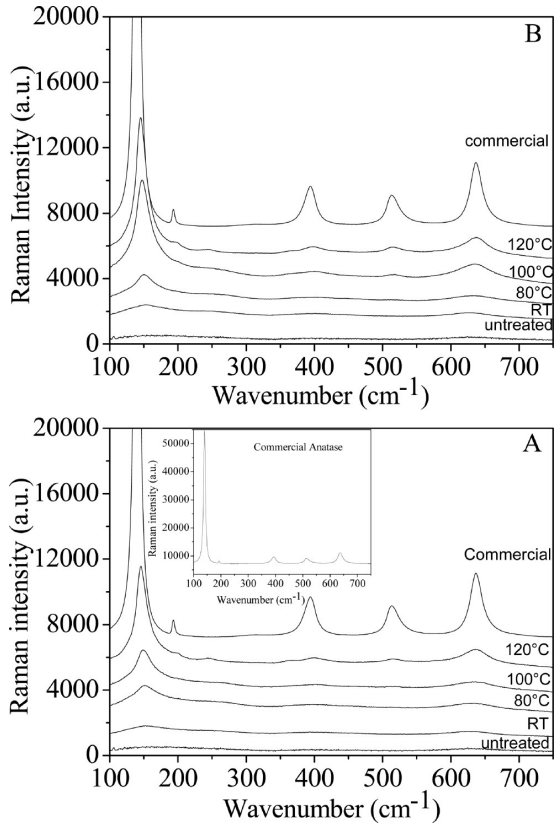

Figure 3. Raman spectra of mesoporous TiO_2 after immersion in water during 8 h (A) or 24 h (B) at different temperatures. Spectrum of commercial anatase with particle size above 20 nm is also given as reference.

vibration due to the anatase is detected on the Raman spectrum before treatment (Figure 3). After immersion during 8 h at room temperature, traces of anatase can be detected on the Raman spectra (Figure 3), in particular the band at 153 cm^{-1}, which is attributed unambiguously to the E_g mode. However, the Raman peaks are broad, and their intensity is rather low, indicating that the titania is not well crystallized, in accordance with the XRD results. By increasing the temperature, the intensity of the Raman vibrations of the water-treated mesoporous titania increases. We can also observe that the E_g mode is shifted to lower wave numbers. For example, after immersion at 100 °C, this band is located at 148 cm^{-1}. The E_g mode provides information about the size of the anatase crystallite.[28,29] The E_g band is located at 146 cm^{-1} for the material plunged in water at 120 °C during 8 h and at 145 cm^{-1} for the titania recovered after 24 h at this temperature,

dx.doi.org/10.1021/sc400323w | ACS Sustainable Chem. Eng. 2014, 2, 120−125

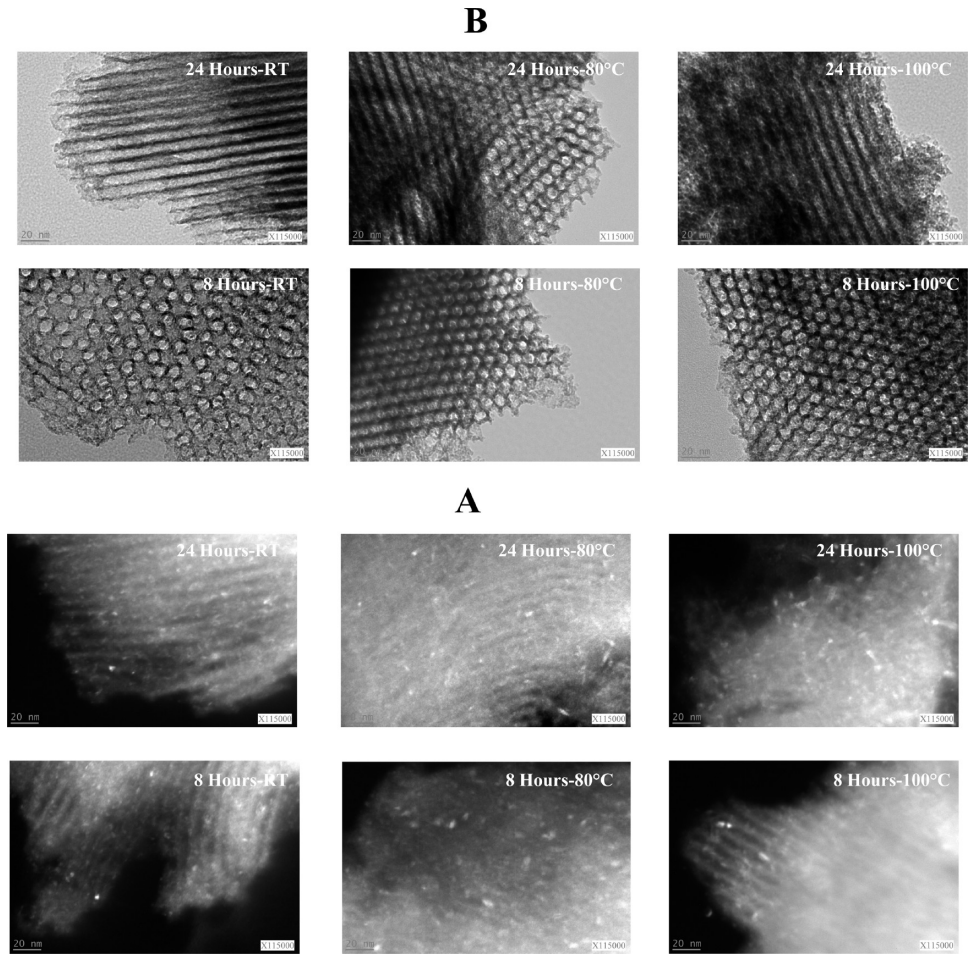

Figure 4. Bright field TEM showing anatase crystallite (A) and TEM micrographs (B) of mesoporous TiO_2 after immersion in water during 8 or 24 h at different temperatures.

confirming the presence of a nanosized crystallite domain when the temperature of the water is raised. The formation of the nanocrystalline anatase particles upon treatment in water is further evidence by the TEM images. As depicted in Figure 4, anatase nanocrystallites are clearly observed on the dark field TEM images (Figure 4A), even after a stay in water at room temperature. Because either the honeycomb like arrangement or the hexagonal stacking of the channels are observed in Figure 4B, it should also be noted that the TEM micrographs support the SAXS results, i.e., that the channel arrangement is preserved after treatment in water.

Two main tendencies can be drawn from the results reported above. First, the hexagonal pore ordering is maintained when the mesostructured titania are immersed in water at room temperature, 80, 100, or 120 °C for short duration (≤1 h); for longer time at this temperature, the mesostructure collapses. Second, during the treatment, nanocrystalline anatase appears. The higher the temperature is, the better the crystallization is. The appearance and the growth of the crystalline structure with temperature thus lead to the loss of mesopore ordering when the treatment at 120 °C is prolonged. Anatase is composed of TiO_6 octahedra sharing faces, and to obtain this structure from amorphous titania, rearrangement of the TiO_6^{2-} octahedral units in the amorphous TiO_2 are necessary. In such a process, water plays a key role. As a matter of fact, in a paper dealing with the crystallization of anatase from amorphous titania using the hydrothermal techniques, Yanagisawa et al.[30] have investigated the mechanism of anatase crystallization from amorphous titania. In their study, the authors have prepared the amorphous TiO_2 by different methods, but never in the presence of surfactant. In addition, no mesopore ordering is obtained. The amorphous to anatase phase transition is catalyzed by water, which adsorbs to the titania surface. In the first step, water molecules form bridges between surface OH groups of different octahedra, which has only one common vertex using the two lone pairs of electrons on the oxygen. Then, dehydration and eventually the addition of a third tetrahedron, driven by water, will involve the formation of the more thermodynamically stable anatase nuclei. Finally, the crystallization of amorphous titania proceeds through a dissolution−precipitation process in which randomly distributed TiO_6^{2-} octahedra are dissolved and rearrange themselves driven by water and precipitate. This dissolution−precipitation process is favored at high temperature.[30] In the same way, Yanagida et al.[31] have also investigated the synthesis of pure anatase by the hydrothermal method under autoclaving conditions at 200 °C by using amorphous TiO_2 as the starting material and various acids as catalysts. They have shown that in the presence of HCl or HF, narrow-sized anatase TiO_2 with regular crystalline surface is obtained, where the use of citric or nitric acid leads to the formation of rutile. More recently, the phase transition induced by water was also exploited by Wang et al.[32] and by Que et al.[33] to develop the crystallization of amorphous titania nanotubes at low temperature. Here, even if

dx.doi.org/10.1021/sc400323w | ACS Sustainable Chem. Eng. 2014, 2, 120−125

no autoclave treatment is performed and no acid is used as catalyst, we can assume that the amorphous walls of mesoporous titania are transformed into anatase according to a similar mechanism than the one propose by Yanagisawa et al.[30] In our case, the phase transition occurs spontaneously. To the best of our knowledge, this is the first time that such a phenomenon is observed for ordered mesoporous titania materials. So, when the mesostructured TiO_2 with amorphous walls is placed in water, the latter catalyzes the nucleation of the anatase phase according to the mechanism described above, even at room temperature. As observed on the XRD spectra, on the Raman spectra and on the TEM images, by increasing the temperature, the crystallinity of titania can be enhanced, and the particles grow. However, at 120 °C, both an increase in the crystallite size and the dissolution−precipitation process, which is accelerated with temperature, involve a complete collapse of the mesostructure if the treatment is prolonged beyond 1 h. The obtained mesoporous titania materials have been tested for the photodegradation of methyl orange. As shown in Figure 5,

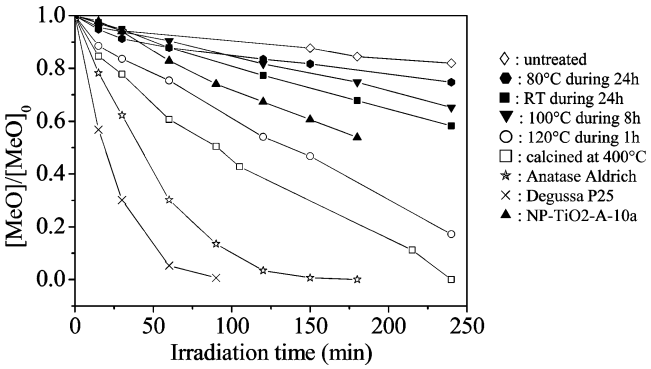

Figure 5. Degradation of methyl orange (MeO) as a function of the time of irradiation of mesoporous TiO_2 after treatment in water at different temperatures, after calcination at 400 °C, and of commercially photocatalysts.

after treatment in water, the photocatalyst efficiency is enhanced. Indeed, for the TiO_2 recovered after 1 h at 120 °C, 85% of methyl orange is degraded with 240 min. The photoactivity can be related to the appearance of anatase.[34] Using a model of pseudo-first-order reaction,[24] the degradation rate (k) has been calculated, and its value varies from 0.005 (1 day at 120 °C) to 0.0017 min^{-1} (24 h at room temperature), depending on the immersion condition time of TiO_2 into water. Usually to transform the amorphous TiO_2 to anatase, calcination is used. So, to investigate the role of crystallinity, we have also compared the efficiency of the photocatalysts recovered after immersion in water and after calcination. To get the mesoporous titania with crystalline walls, the amorphous TiO_2 was calcined at 400 °C under the same conditions previously reported.[23] In addition, the photocatalytic activity of the highly ordered mesoporous titania has been compared with the one of the commercial photocatalysts. Degussa P25 (70% anatase, 30% rutile, and 50 m^2 g^{-1} BET surface area), Nanopowder [NP−TiO_2−A−10a TiO_2 (anatase, 99%, 10 nm, and 210 m^2 g^{-1} BET surface area)] from MTI Corporation, and anatase from Aldrich (25 nm and 45−55 m^2 g^{-1} BET surface area) have been considered. From Figure 5, we can see that P25 and TiO_2 anatase from Aldrich show superior photocatalytic efficiency compared to the mesoporous TiO_2 arising from the crystallization under treatment in water. Even if its specific surface area is lower (165 m^2/g BET surface area), a similar tendency is obtained with calcined TiO_2. As a matter of fact, in that case, about 100% of the dye is degraded within 240 min. This confirms that the degree of crystallinity of TiO_2 is a key parameter for the design of photocatalyst. However, it should be noted that Nanopowder (NP−TiO_2−A−10a TiO_2) has a lower activity. This shows that the photocatalyst efficiency depends also on the size of the particles.

CONCLUSIONS

Ordered mesoporous TiO_2 with a semi-crystalline framework has been prepared by a green, relatively simple, and effective method without post-treatment. The anatase structure is obtained by phase transformation of amorphous TiO_2 in water. The Raman, DRX, and TEM analyses show that the phase transformation can occur even at room temperature. The formation of anatase is favored when the temperature is increased; however, if the immersion at 120 °C is higher than 1 h, the mesopore ordering is lost.

ASSOCIATED CONTENT

Supporting Information

Figures showing the variation of the nitrogen adsorption−desorption isotherm, mesopore size distribution (S1), and specific surface area (S2) with the immersion time and temperature. This material is available free of charge via the Internet at http://pubs.acs.org.

AUTHOR INFORMATION

Corresponding Author

*Tel: + 33 3 83 68 43 70. Fax: + 33 3 83 68 43 44. E-mail: Jean-Luc.Blin@univ-lorraine.fr.

Notes

The authors declare no competing financial interest.

REFERENCES

(1) Ren, Y.; Ma, Z.; Bruce, P. G. Ordered mesoporous metal oxides: Synthesis and applications. *Chem. Soc. Rev.* **2012**, *41*, 4909−4927.
(2) Rao, Y.; Antonelli, D. M. Mesoporous transition metal oxides: Characterization and applications in heterogeneous catalysis. *J. Mater. Chem.* **2009**, *19*, 1937−1944.
(3) Hoffmann, M.; Martin, S.; Choi, W.; Bahnemann, D. Environmental applications of semiconductor photocatalysis. *Chem. Rev.* **1995**, *95*, 69−96.
(4) Fox, M.; Dulay, M. Heterogeneous photocatalysis. *Chem. Rev.* **1993**, *93*, 341−357.
(5) Linsebigler, A.; Lu, G.; Yates, J. Photocatalysis on TiO_2 Surfaces: Principles, mechanisms, and selected results. *Chem. Rev.* **1995**, *95*, 735−758.
(6) Thurston, T.; Wilcoxon, J. Photooxidation of organic chemicals catalyzed by nanoscale MoS_2. *J. Phys. Chem. B* **1999**, *103*, , 11−17.
(7) Chen, X.; Mao, S. S. Titanium dioxide nanomaterials: Synthesis, properties, modifications, and applications. *Chem. Rev.* **2007**, *107*, 2891−2959.
(8) Pelizzetti, E.; Minero, C.; Borgarello, E.; Tinucci, L.; Serpone, N. Photocatalytic activity and selectivity of titania colloids and particles prepared by the sol-gel technique: Photooxidation of phenol and atrazine. *Langmuir* **1993**, *9*, 2995−3001.
(9) Ohtani, B.; Ogawa, Y.; Nishimoto, S. Photocatalytic activity of amorphous-anatase mixture of titanium(IV) oxide particles suspended in aqueous solutions. *J. Phys. Chem. B* **1997**, *101*, 3746−3752.
(10) Kelly, S.; Pollak, F. H.; Tomkiewicz, M. Raman spectroscopy as a morphological probe for TiO_2 aerogels. *J. Phys. Chem. B* **1997**, *101*, 2730−2734.

(11) Zhang, W. F.; He, Y. L.; Zhang, M. S.; Yin, Z.; Chen, Q. Raman scattering study on anatase TiO_2 nanocrystals. *J. Phys. D: Appl. Phys.* **2000**, *33*, 912−916.
(12) Yang, P.; Zhao, D.; Margolese, D. I.; Chmelka, B. F.; Stucky, G. D. Generalized syntheses of large-pore meosporous metal oxides with nanocrystalline walls. *Nature* **1998**, *396*, 152−154.
(13) Ismail, A. A.; Bahnemann, D. W. Mesoporous titania photocatalysts: Preparation, characterization and reaction mechanisms. *J. Mater. Chem.* **2011**, *21*, 11686−11707.
(14) Zhang, R.; Elzatahry, A. A.; Al-Deyab, S. S. Mesoporous titania: From synthesis to application. *Nano Today* **2012**, *7*, 344−366.
(15) Antonelli, M. M.; Ying, J. Y. Synthesis of hexagonally packed mesoporous TiO_2 by a modified sol-gel method. *Angew. Chem., Int. Ed. Engl.* **1995**, *34*, 2014−2017.
(16) Tian, B.; Liu, X.; Tu, B.; Yu, C.; Fan, J.; Wang, L.; Xie, S.; Stucky, G. D.; Zhao, D. Self-adjusted synthesis of ordered stable mesoporous minerals by acid-base pairs. *Nat. Mater.* **2003**, *2*, 159−163.
(17) Tian, B.; Yang, H.; Liu, X.; Xie, S.; Yu, C.; Fan, J.; Tu, B.; Zhao, D. Fast preparation of highly ordered nonsiliceous mesoporous materials via mixed inorganic precursors. *Chem. Commun.* **2002**, 1824−1825.
(18) Li, H.; Shi, J. L.; Liang, J.; Li, X.; Li, L.; Ruan, M. Synthesis of well-ordered mesoporous titania powder with crystallized framework. *Mater. Lett.* **2008**, *62*, 1410−1413.
(19) Sung, C. C.; Fung, K. Z.; Hung, I. M.; Hon, M. H. Synthesis of highly ordered and worm-like mesoporous TiO_2 assisted by tri-block copolymer. *Solid State Ionics* **2008**, *179*, 1300−1304.
(20) Shibata, H.; Ogura, T.; Ohkubo, T.; Sakai, H.; Abe, M. Direct synthesis of mesoporous titania particles having a crystalline wall. *J. Am. Chem. Soc.* **2005**, *127*, 16396−16397.
(21) Kao, L. H.; Hsu, T. C.; Cheng, K. K. Novel synthesis of high-surface-area ordered mesoporous TiO_2 with anatase framework for photocatalytic applications. *J. Colloid Interface Sci.* **2010**, *341*, 359−365.
(22) Zimny, K.; Ghanbaja, J.; Carteret, C.; Stébé, M. J.; Blin, J. L. Highly ordered mesoporous titania with semi crystalline framework templated by large or small nonionic surfactants. *New. J. Chem.* **2010**, *34*, 2113−2117.
(23) Zimny, K.; Roques-Carmes, T.; Carteret, C.; Stébé, M. J.; Blin, J. L. Synthesis and photoactivity of ordered mesoporous titania with a semicrystalline framework. *J. Phys. Chem. C* **2012**, *116*, 6585−6594.
(24) Blin, J. L.; Stébé, M. J.; Roques-Carmes, T. Use of ordered mesoporous titania with semi-crystalline framework as photocatalyst. *Colloids Surf., A* **2012**, *407*, 177−185.
(25) Sing, K. S. W.; Everett, D. H.; Haul, R. A. W.; Moscou, L.; Pierotti, R. A.; Rouquerol, J.; Siemieniewska, T. Reporting physisorption data for gas/solid systems with special reference to the determination of surface area and porosity (recommendations 1984). *Pure Appl. Chem.* **1985**, *57*, 603−619.
(26) Barret, E. P.; Joyner, L. G.; Halenda, P. P. The determination of pore volume and area distributions in porous substances. I. Computations from nitrogen isotherms. *J. Am. Chem. Soc.* **1951**, *73*, 373−380.
(27) Klug, H. P. and Alexander, L. E. In *X-ray Diffraction Procedures*; Wiley: New York, 1954; Chapter 9.
(28) Kelly, S.; Pollak, F. H.; Tomkiewicz, M. Raman spectroscopy as a morphological probe for TiO_2 aerogels. *J. Phys. Chem. B* **1997**, *101*, 2730−2734.
(29) Zhang, W. F.; He, Y. L.; Zhang, M. S.; Yin, Z.; Chen, Q. Raman scattering study on anatase TiO_2 nanocrystals. *J. Phys. D: Appl. Phys.* **2000**, *33*, 912−916.
(30) Yanagisawa, K.; Ovenstone, J. Crystallization of anatase from amorphous titania using the hydrothermal technique: Effects of starting material and temperature. *J. Phys. Chem. B* **1999**, *103*, 7781−7787.
(31) Yin, H.; Wada, Y.; Kitamura, T.; Kambe, S.; Murasawa, S.; Mori, H.; Sakata, T.; Yanagida, S. Hydrothermal synthesis of nanosized anatase and rutile TiO_2 using amorphous phase TiO_2. *J. Mater. Chem.* **2001**, *11*, 1694−1703.
(32) Wang, D.; Liu, L.; Zhang, F.; Tao, K.; Pippel, E.; Domen, K. Spontaneous phase and morphology transformations of anodized titania nanotubes induced by water at room temperature. *Nano Lett.* **2011**, *11*, 3649−3655.
(33) Liao, Y.; Que, W.; Zhong, P.; Zhang, J.; He, Y. A facile method to crystallize amorphous anodized TiO_2 nanotubes at low temperature. *ACS Appl. Mater. Interfaces* **2011**, *3*, 2800−2804.
(34) Sreethawong, T.; Suzuki, Y.; Yoshikawa, S. Photocatalytic evolution of hydrogen over nanocrystalline mesoporous titania prepared by surfactant-assisted templating sol-gel process. *Catal. Commun.* **2005**, *6*, 119−124.